Journal of the European Ceramic Society **5** (1989) 201–205

Tensile and Compressive Creep Characteristics from Bending Tests: Application to SiC–SiC Composites

François Abbé, Régis Carin & Jean-Louis Chermant

LERMAT, URA CNRS No. 1317, ISMRa - Université, Boulevard du Maréchal Juin, 14032 Caen Cedex, France

(Received 12 June 1989; revised version received 4 September 1989; accepted 15 September 1989)

Abstract

Tensile tests can be performed on ceramic materials, but many experimental difficulties arise when tests are performed at very high temperature. In this paper we used the analysis provided by Chuang to obtain tension and compression data from bending tests. Good agreement has been obtained in the case of creep investigations of fiber-reinforced ceramic matrix composite materials, such as SiC–SiC.

Das Zugprüfungsverfahren kann an keramischen Werkstoffen durchgeführt werden, es treten aber viele experimentelle Schwierigkeiten auf, wenn die Versuche bei sehr hohen Temperaturen durchgeführt werden. Aus diesen Gründen verwendeten wir das von Chuang aufgestellte Analysenverfahren, um die Spannungs- und Kompressionsdaten aus Biegeversuchen zu berechnen. Im Falle von Kriechexperimenten an faserverstärkten Keramikkompositen wurde eine gute Übereinstimmung gefunden.

Les matériaux céramiques peuvent être testés en traction, mais à haute température surgissent de nombreuses difficultés expérimentales pour effectuer ce type d'essais mécaniques. Dans cet article, nous avons utilisé l'analyse proposée par Chuang pour obtenir les données de traction et de compression à partir d'essais de flexion. Une bonne corrélation et de bons résultats ont ainsi été obtenus dans le cas de l'étude en fluage de matériaux composites céramiques à fibres longues: SiC–SiC.

1 Introduction

Fiber-reinforced ceramic matrix composites (FRCMC) seem to be the best candidate for applications in structural components, because of their ability to withstand high temperature as well as their high resistance to environmental and chemical corrosion, and above all their strength combined with toughness due to fiber incorporation. To use FRCMC in such applications, the design engineer has to be able to predict the long-term behavior of these materials at high temperature and then to utilize creep data.

Although flexural tests are most commonly used to investigate creep behavior of ceramic materials,[1] several investigations[2–6] have pointed out discrepancies, due to the stresses redistribution in such specimens. However, creep tests in bending are carried out because of the simple geometry of the specimen required. Moreover, the experimental procedure is easier to perform because it avoids problems of complex shape for specimens, gripping and alignment of samples, which more specifically belong to the tensile test in the case of ceramic materials. Thus some authors focused their attention on estimating creep parameters in tension and compression from bending tests. Finnie[2] was the first to present a method to predict creep in tension and compression from bending tests, using trapezoidal specimens and the power law creep hypothesis ($n = 1$). Talty and Dirks[4] extended Finnie's analysis of trapezoidal sample to the case of a stress exponent different from unity. More recently, Chuang[6] extended this analysis to a completely general case, where the pre-exponent factors and also stress exponents of tension and compression creep behavior laws are distinct.

The aim of this paper is to present the applicability, by a specific method, of a flexural creep data deconvolution to obtain indirectly tension or compression data for designers.

2 Theoretical Background

Ceramics often present damage-enhanced creep, especially in tension[7] and different behavior in compression than in tension. From the first analysis[8] on SiC–SiC materials, the present authors have been engaged in using a methodology originally developed by Cohrt *et al.*[3] and adapted by Chuang, that will be briefly summarized. The reader can refer for more details to Refs 6 and 9.

The different behavior in tension and compression is the starting point for the Cohrt[3] and Chuang[6,9] analyses: the widely used Norton law is then divided in two parts, one for compression and the other one for tension, with a λ ratio. The physical meaning of λ corresponds to the fact that creep rate in compression is λ times the creep rate in tension, for the same stress value. However, for certain materials, such as ceramics or ceramic composites, damage occurs and must be taken into consideration: above a given threshold stress there is a large increase in the stress exponent. So the mechanical behavior law for the steady state is made of two different parts, corresponding to tension and compression, with a bimodal behavior for the tensile characteristics, to account for the damaging effect. The position of the neutral axis moves through the initial region of compression as far as the loading occurs. The following expressions can then be used:

$$\text{tensile creep} \begin{cases} \dot{\varepsilon}_s = \dot{\varepsilon}_0 \left(\dfrac{\sigma}{\sigma_0}\right)^n & \text{for } \sigma \le \sigma_0 \\ \dot{\varepsilon}_s = \dot{\varepsilon}_0 \left(\dfrac{\sigma}{\sigma_0}\right)^N & \text{for } \sigma > \sigma_0 \end{cases}$$

$$\text{compressive creep } |\dot{\varepsilon}_s| = \lambda \dot{\varepsilon}_0 \left(\frac{\sigma}{\sigma_0}\right)^n$$

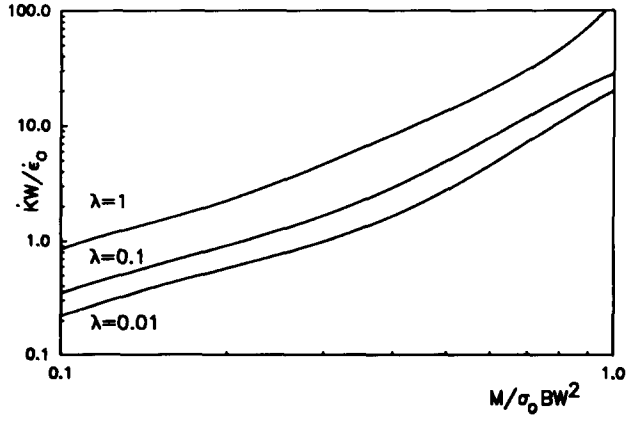

Fig. 1. Normalized curvature rate as a function of the normalized applied moment for different values of the tensile–compressive ratio λ. $\dot{K}$ is the curvature rate, W the thickness of the specimen, $\dot{\varepsilon}_0$ the strain rate, M the applied moment, σ_0 the threshold stress, B the specimen width.

where $\dot{\varepsilon}_s$ is the steady-state creep rate and $\dot{\varepsilon}_0$ is the creep rate at the threshold stress σ_0, with $N > n$ (N and n being the stress exponents), and λ is the ratio of compressive to tensile creep rates. The tension part is split into two behavior laws, providing a threshold stress above which damage occurs. Chuang obtained a good agreement from his bending analysis with respect to direct tensile and compressive tests. So the knowledge of n, N and λ allows the correct description of the behavior of such ceramic materials in bending for steady-state conditions. The $\dot{\varepsilon}_s$–σ_a plot is then translated in a $\dot{k}$–m (normalized curvature rate–normalized applied moment) using the following relationships:

$$\sigma_a = \frac{6M}{BW^2} \qquad m = \frac{M}{\sigma_0 BW^2}$$

$$\dot{\varepsilon}_s(y) = \dot{K}Wy \qquad \dot{k} = \frac{\dot{K}W}{\dot{\varepsilon}_0}$$

where σ_a is the applied stress, M the applied moment, W the specimen thickness, B the specimen width, σ_0 the threshold stress, $\dot{\varepsilon}_s$ the strain rate at a y location from the neutral axis, $\dot{K}$ the curvature rate and $\dot{\varepsilon}_0$ the creep rate at the threshold stress. This change in variable allows freedom from $\dot{\varepsilon}_0$ and σ_0 in a first step, but requires the knowledge of the neutral axis position to establish, from n, N and λ, the relationship between $\dot{k}$ and m.

The neutral axis location is solved using the following equilibrium equation:

$$\int_A \sigma \, dA = 0$$

As the calculations provided by Chuang in his paper are constructed with n, N and λ different from our values, his theoretical background has been reanalyzed. The equations were computed in PASCAL language and solved using a Newton–Raphson algorithm to obtain the neutral axis location value. Figure 1 presents some of the results for different λ values.

In this work, the λ value was determined from the location of the neutral axis. The neutral axis measurement was achieved from the measurement of the distance L between two marks of deposited refractory material on the polished side surface of the specimen (Fig. 2). The fiber strain at each beam location was calculated as follows:

$$\varepsilon = (L - L_0)/L_0$$

Thus the ratio of compressive to tensile creep rate, λ, was simply deduced from the measurements of the neutral axis ($\varepsilon = 0$) location (see Fig. 2), x,[10] for a test

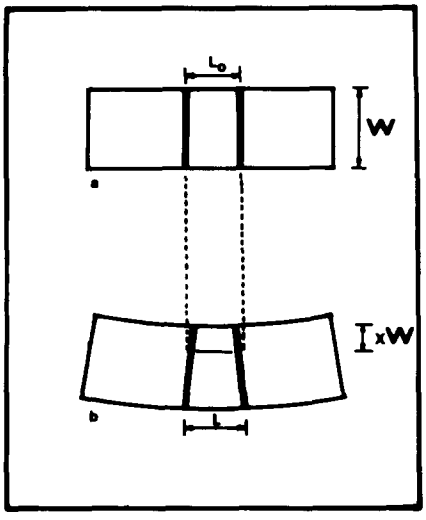

Fig. 2. Scheme of the specimen before (a) and after (b) the creep test in bending.

conducted in the stress–strain zone where damage does not occur.[3] In this case, λ is given by:

$$\lambda = \left(\frac{x}{1-x}\right)^{n+1} \qquad \text{for } (\sigma < \sigma_0)$$

3 Materials and Experimental Method

For this investigation, as an example, SiC–SiC composite materials (batches developed as model materials) made by the Société Européenne de Propulsion (SEP, Etablissement de Bordeaux, France) were used. The composites are made of a two-dimensional cloth of Nicalon SiC fibers[11] and a SiC matrix obtained from a chemical vapor infiltration process. These composite materials can be described from their planar section as an array of three phases: the fibers, the matrix and the pores. Morphological characteristics and quantitative measurements have been done previously[12,13] giving size distribution of SiC fibers, porosity values and radial size distribution of fibers using automatic image analysis.

Creep investigations were carried out under vacuum ($\sim 10^{-4}$ Pa) using the three-point bending test (bending span of 14 mm) in a Sesam opening furnace (VMDI, France). Constant loading was achieved by using a lever arm and a dead weight acting on the upper push rod, made of tungsten with cylindrical knives in titanium carbide. Displacement was measured using linear variable differential transducers (LVDT). A displacement of 1 μm can be measured accurately. The load was always applied perpendicularly to the SiC cloth. A description of the device is presented in Ref. 14. The specimens used are 20 mm long, 9·5 mm wide and 2·5 mm thick.

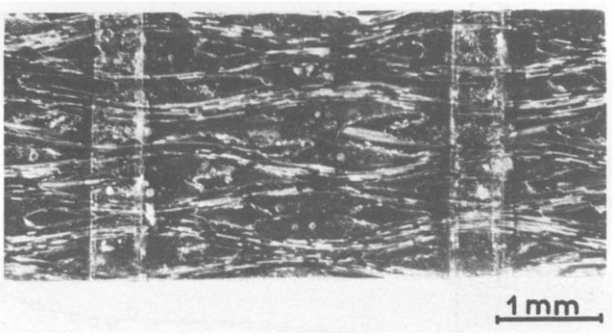

Fig. 3. Macrograph of a SiC–SiC specimen with two marks before the creep experiment.

The two marks were deposited on the specimen surface by reactive sputtering, using a mask method.[15] The refractory material (AlN) was obtained by sputtering of an aluminum target with nitrogen ions in a radio-frequency (diode-type) discharge apparatus.[16] The deposition was performed on the water-cooled specimen, at a N_2 pressure of 1·3 Pa. The distance between the target and the sample was 35 mm and the voltage 2 kV.

Figure 3 presents the macrograph of a specimen of SiC–SiC, with two straight marks in AlN to perform the proposed deconvolution analysis.

4 Results and Discussion

First of all, it was verified that, for each creep experiment, steady-state strain rate occurs (Fig. 4). The quasi-steady state is assumed when the creep rate reaches a minimum value. For this investigation, tests were performed at 1573 K and 1473 K, under a vacuum of 10^{-4} Pa, for about 100 h, with a stress range up to 200 MPa. Steady-state creep rates versus the outer fiber stress are presented in Fig. 5.[8]

From these experimental results and using the Chuang analysis, the N, n and λ parameters have been determined: λ from the change in the distance between the two refractory marks, and N and n from the slopes of the $\dot{\varepsilon}$–σ_a plot. The values used for the Chuang analysis are reported in Table 1.

The knowledge of N, n and λ parameters allows the representation of the normalized curvature rate versus normalized moment function. $\dot{\varepsilon}_0$ and σ_0 are thus determined using the experimental data. The theoretical curves deduced for these parameters from the Chuang model were compared with experimental data, transformed into curvature moment values. It can be seen that the results, for example at 1573 K (data points on Fig. 6), agree with the Chuang model (solid line on Fig. 6).

The values used for $\dot{\varepsilon}_0$ and σ_0 are given in Table 2.

Values for σ_0 and $N > n$ have been introduced to

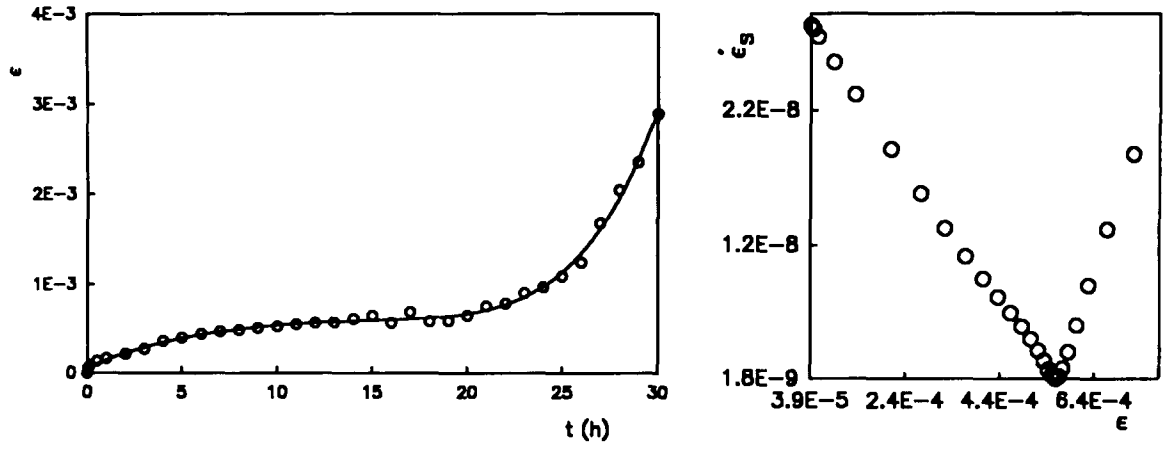

Fig. 4. Example of the quasi-steady state strain rate determination $\varepsilon(t)$ curve and corresponding $\dot{\varepsilon}_s = f(\varepsilon)$ plot.

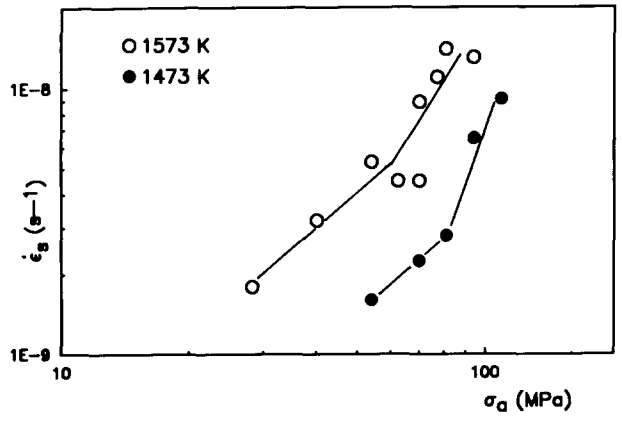

Fig 5. Experimental results of strain rate, $\dot{\varepsilon}$, as a function of the outer fiber stress, σ_a, for SiC–SiC materials, crept at 1573 K and 1473 K.

Table 1. Experimental values used for the three Chuang parameters for tests run at 1573 K and 1473 K

$T(K)$	N	n	λ
1 573	3·2	1·4	0·14
1 473	5·6	1·4	0·14

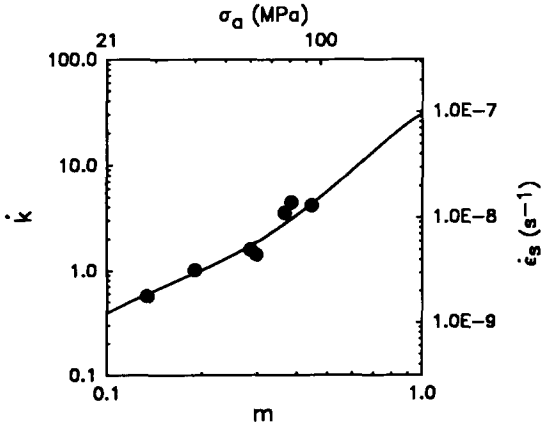

Fig. 6. Normalized curvature rate, $\dot{K}$, as a function of normalized applied moment, $M/\sigma_0 BW^2$. The solid line corresponds to the model (with $\lambda = 0{\cdot}14$) and the points are experimental data.

characterize a more rapid creep beyond a certain threshold stress. The preponderant mechanism is a localized damage in the tensile zone of the bending specimen. For example, in the case of siliconized silicon carbide composites (particulate composites, Si–SiC, made by SOHIO Corp., Cleveland, Ohio), investigated by the team of Wiederhorn and Chuang,[7-9] these authors have shown that the threshold stress is related to a cavitation phenomenon, which occurs for stresses greater than the threshold stress σ_0.

Table 2. Values of the strain rate, $\dot{\varepsilon}_0$, and the threshold stress, σ_0, from bending tests, and of the threshold stress obtained directly from tensile test, σ_{ot}, for experiments performed at 1573 and 1473 K

$T(K)$	$\dot{\varepsilon}_0(s^{-1})$	$\sigma_0(MPa)$	$\sigma_{ot}(MPa)$
1 573	$4{\cdot}5\ 10^{-9}$	36	~40
1 473	$2{\cdot}8\ 10^{-9}$	50	~60

In this case, for SiC–SiC materials with long ceramic fibers, the threshold stress can be compared to the one above, in which damage occurs during tensile tests.[17] A good agreement between these two types of data (Table 2) is observed. It indicates that the threshold stress, beyond which the creep is more sensitive to the strain, also corresponds to a threshold beyond which initiation of SiC matrix microcracking arises.

5 Conclusion

The use of the deconvolution method based on a damage-enhanced creep model, proposed by Chuang and initially developed for two-phase particulate composites, gives data from the bending creep test in compression and in tension. This

method was extended to long fiber-reinforced ceramic matrix composites, which also present bilinear behavior.

This analysis contains several features of the creep behavior of ceramics: higher creep rates in tension than in compression and higher stress exponents at higher stresses, leading to higher creep rates from both tension and bending tests. It points out the shift of the neutral axis towards the compression side of the specimen submitted to bending tests. The parameters introduced in the analysis[6] are determined experimentally. Thus deconvolution of the bending creep test is achieved from neutral axis measurements and the damage-enhanced creep model.

Thus the applicability of such analysis for ceramic materials reinforced with long ceramic fibers has been confirmed and the threshold stress introduced has been correlated with the one obtained from tension data.

Acknowledgments

Part of this work has been performed under the BRITE Program of the European Commission, Project P-1348-6-85, Contract RI 1B-0098. The authors wish to thank SEP Company, Etablissement de Bordeaux, for its help in this investigation.

References

1. Cannon, W. R. & Langdon, T. G., *J. Mater. Sci.*, **18** (1983) 1–50.
2. Finnie, I., *J. Amer. Ceram. Soc.*, **49** (1966) 218–20.
3. Cohrt, H., Grathwohl, G. & Thümmler, F., *Res. Mechanica Lett.*, **1** (1981) 159–64.
4. Talty, P. K. & Dirks, R. A., *J. Mater. Sci.*, **13** (1978) 580–6.
5. Fett, T., Keller, K. & Munz, D., *J. Mater. Sci.*, **23** (1988) 467–74.
6. Chuang, T. J., *J. Mater. Sci.*, **21** (1986) 165.
7. Wiederhorn, S. M., Roberts, D. E., Chuang, T. J. & Chuck, L., *J. Amer. Ceram. Soc.*, **71** (1988) 602–8.
8. Abbé, F., Vicens, J. & Chermant, J. L., *J. Mater. Sci. Lett.*, **8** (1989) 1026–8.
9. Chuang, T. J. & Wiederhorn, S. M., *J. Amer. Ceram. Soc.*, **71** (1988) 595–601.
10. Chen, C. F. & Chuang, T. J., *Ceram. Eng. Sci. Proc.*, **8** (1987) 796–804.
11. Dauchier, M., Lamicq, P. & Macé, J., *Rev. Int. Htes Temp. Réfract. Fr.*, **19** (1982) 285–99.
12. Abbé, F., Chermant, L., Coster, M. & Chermant, J. L., Report, Contract DRET-SEP, No. 85-528, March 1989.
13. Abbé, F., Chermant, L., Coster, M., Gomina, M. & Chermant, J. L., *Comp. Sci. Tech.*, **37**(1–3) (1989) 109–27.
14. Fourvel, P., Gomina, M., Abbé, F., Osterstock, F. & Chermant, J. L., Report BRITE, Project No. P 1348-6-85, Contract RI 1B-0098, July 1988.
15. Abbé, F., Rapport DEA, CEA-CEN-SACLAY/D. TECH/SRMP, 1987.
16. Carin, R., Elaboration et étude des couches minces isolaites de nitrune de gallium pour la passivation de l'arséniune de gallium. Thèse de Doctorat ès Sciences, Caen, 1989.
17. Choury, J. J., Thermostructural composite materials in aeronautics and space applications. *French Aerospace 1989 Aeronautical and Space Conference*, Delhi, 15–17 February 1989 and Bangalore, 20–22 February 1989.